

# Evaluation of the Critical Load Parameter: Prediction of voltage collapse under steady state system operation

Oladeji I. R

Electrical and Electronics Engineering Department  
Federal University of Technology, Akure  
daystarclub@yahoo.com

Oyinlola A. O

Electrical and Electronics Engineering Department  
Federal University of Technology, Akure  
wumgold@yahoo.com

## Abstract

The number of occurrence of power system blackouts as a result voltage collapse due to the operation of power systems close to their thresholds is on the increase annually. This paper presents the results of implementation of formulated algorithms to predict the event of voltage collapse using the load parameter. The critical load parameter of the modified IEEE 14 bus network is determined using continuous power flow Gauss Seidel algorithm developed and implemented on PSAT 2.19 toolbox on Matlab. An index of 1.522p.u and 1.61p.u was obtained using bus 1 and bus 2, 3, 6 and 8 as slacks respectively. The distance to instability can be increased by line reinforcements, implementation of FACTS devices and use of on-load tap changers, fast governor action and load shedding scheme.

**Key words-**Voltage Collapse, Steady state, Critical Load Parameter, Continuous Power flow.

## I. INTRODUCTION

Power systems are predominantly in the steady state operation mode. They are planned, designed and built to supply consumers with steady electrical energy considering supply quality, economic impact and supply security. Under steady state operation, these quantities are well under limits even in the case of small and gradual change in MW loading and disturbances. However, when the disturbance is large and sudden, the system must be monitored to prevent going into collapse. Voltage collapse is the total loss of voltage or the presence of voltage so much beyond the statutory limit in some or all the buses within the network. Figure 1 shows the critical loading point of operation during which voltage collapse occur. Steady state stability refers to the ability of the power system to remain in synchronism with elements within and outside itself when subjected to small disturbances. It is safe to assume that disturbances causing the changes disappear over time [5].

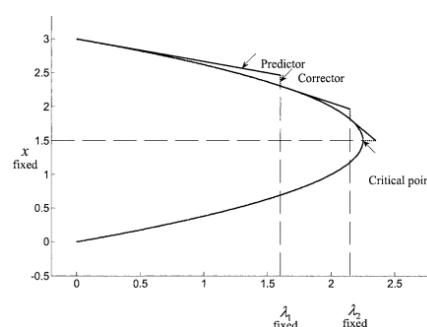


Figure 1 Critical Load Parameter

A Critical load parameter  $\lambda$ , corresponds to the MW loading of the network beyond which steady state stability cannot be maintained [1]. The voltage corresponding to this critical load parameter is known as the critical voltage. Appropriate actions must be taken to prevent the operation of power systems close to this critical point.

### A. Power system states

The state/operation of a power system lies in the normal region most of the time. System parameters are within the normal range and no equipment is overstressed. The alert state is close to the normal state except that the above conditions cannot be met in case of disturbance. However in alert region, all system parameters are within the normal range and all constraints are yet satisfied. The system transits into the emergency state at the occurrence of a major disturbance. Transient disturbance would always likely lead the system into a state of in-extremis where blackouts occur. The restorative state is a transition state between the in-extremis and the normal state [6]. This transition must be secure and quick so as to prevent the spread of the effect of power system blackouts. Quick faults clearing, excitation/voltage control, fast valving, generator tripping, load shedding, implementation of FACTS devices and HVDC are ways to maintain the system in the normal and alert states [12].

**B. Voltage stability and Rotor angle stability**

The total active electrical power fed into the power system by the generators is always equal to the active power consumed by the loads including the losses in the system. On the other hand, there is not always a similar balance between the loads and the power fed into the generators by the prime movers, e.g. the hydro and steam turbines. If such an imbalance develops, the rotating parts of the generators and other rotating machines will act as energy buffer, and the kinetic energy stored in these will decrease or increase as a result of the imbalance. Figure 2 shows the OMIB network model relating the total generated and consumed active and reactive powers respectively.

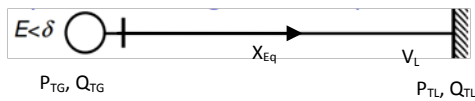


Figure 2 One Machine Infinite Bus Model (OMIB)

Rotor angle stability refers to the ability of synchronous machines of a power system to remain in synchronism after a disturbance [13]. However, when it comes to reactive power balance the situation is not as clear and simple as concerning active power. There is always a balance between “produced” and “consumed” reactive power in every node of a network. Whenever there is imbalance in the reactive power at a bus or in the network altogether, then voltage instability issues develop. If the operating condition is not closely monitored the bus voltages would go beyond acceptable range and thereafter voltage collapse may occur. Voltage stability problems are localised at the load buses while rotor angle stability is related to the system generators.

**II. PROBLEM FORMULATION AND RESEARCH METHODOLOGY**

**A. Steady state power flow**

Power flow study, commonly referred to as load flow is essential for power system planning, design, analysis and operation. The main objectives of power flow studies are to obtain the voltage magnitudes and voltage angles at each nodes, the current flow through the line, line losses, and reactive powers at each generator buses. Power flow studies are also required for transient stability and dynamic stability problems analysis. Considering an *i*th bus of the network as shown in Figure 3, the total injected current *I<sub>i</sub>* into the bus is given as:

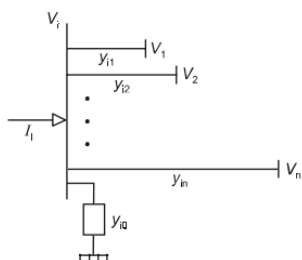


Figure 3 An *i*th Bus of a Power System

$$I_i = Y_{i0}V_i + Y_{i1}(V_i - V_1) + Y_{i2}(V_i - V_2) + \dots + Y_{in}(V_i - V_n) \tag{1}$$

$$I_i = Y_{ii}V_i + \sum_{k=1}^n Y_{ik}V_k \tag{2}$$

where *V* is the bus voltage, *Y* is the bus admittance and *Y<sub>i0</sub>* is the total charging admittance at bus *i*.

The real and reactive power at the *i*th bus is evaluated as

$$P_i - jQ_i = V_i^* I_i \tag{3}$$

Then substituting for *I<sub>i</sub>*

$$\frac{P_i - jQ_i}{V_i^*} = Y_{ii}V_i + \sum_{k=1}^n Y_{ik}V_k \tag{4}$$

Therefore the bus voltage is given as

$$V_i = \frac{1}{Y_{ii}} \left[ \frac{P_i - jQ_i}{V_i^*} - \sum_{k=1}^n Y_{ik}V_k \right] \tag{5}$$

The above equation for multimachine system can only be solved using iterative methods [3]. Newton Raphson and Gauss Seidel methods are the most common of all numerical iteration/approximation methods available.

For P-Q buses, the real and reactive powers *P<sub>i</sub>* and *Q<sub>i</sub>* are known. Beginning with the initial guess values of the bus voltages, the set of equations can be solved iteratively. Furthermore considering the P-V buses where the *P<sub>i</sub>* and *V<sub>i</sub>* are known, the *Q* at the *i*th bus is calculated from

$$Q_i^{n+1} = - \sum_{k=1}^n V_i^n V_k^n Y_{ik} \sin(\theta_{ik} - \delta_i^n + \delta_k^n) \tag{6}$$

Numerical solution methods for determining the bus voltages where the previous value is replaced by the new solution is employed until the difference between the previous values and the last values are within a specified accuracy  $\epsilon$  as defined by

$$\Delta V = \max |V_i^{(n+1)} - V_i^{(n)}|, \quad i = 1, 2, \dots, n \tag{7}$$

where  $\Delta V$  is the change in bus voltage.

If  $\Delta V \leq \epsilon$ , then the solution is then said to converge.

Also in terms of real and active power,

$$\Delta P = \max |P_i^{calculated} - P_i^{scheduled}| \tag{8}$$

$$\Delta Q = \max |Q_i^{calculated} - Q_i^{scheduled}| \tag{9}$$

where  $\Delta P$  and  $\Delta Q$  are real and reactive power mismatches respectively. Again if  $\Delta P \leq \epsilon$  and  $\Delta Q \leq \epsilon$ , then the solution has converged [3].

**B. Power Voltage Curve**

The power - voltage (PV) curve which often refers to the overall network voltage response at a particular bus to MW load increment in a certain area or bus is shown in Figure 4. The upper portion of the PV curve depicts the stable solution where the system bus voltages lie within acceptable range and the drooping part of the curve represents the load dynamics curve and the unstable region.

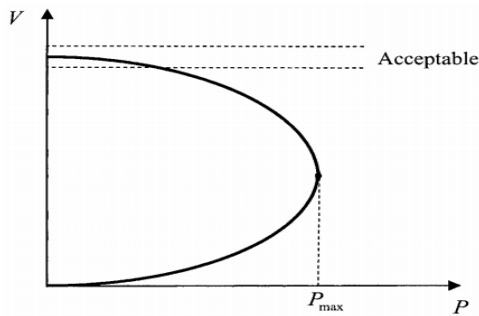


Figure 4 P-V Curve showing Maximum Power

The PV curve is useful for analysing voltage stability margins and network loadability with the aim of preventing blackouts and voltage collapse. Considering a SMIB power transmission system of reactance  $jX$ , generator terminal voltage  $V_1$ , infinite bus voltage  $V_2$ , active and reactive power  $P$  and  $Q$  as shown in Figure 5,

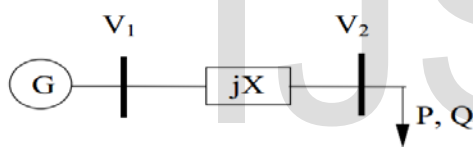


Figure 5 Simple Power Transmission System

the power voltage characteristics between the buses 1 and 2 obtained through the implementation of continuous power flow is governed by the equation given as [2];

$$V_2 = \sqrt{\frac{(V_1^2 - 2QX) \pm \sqrt{V_1^4 - 4QXV_1^2 - 4P^2X^2}}{2}} \quad 10$$

**C. Continuous Power Flow**

The continuous power flow technique is a robust power flow method that can ensure convergence at the voltage collapse point (nose point) and unstable equilibrium points on the lower portion of a P-V curve. Therefore, this technique can be used to predict voltage instability by identifying the collapse point or critical load parameter. The load parameter variable  $\lambda$  is introduced into the conventional power flow equations to obtain;

$$P_{G_{i0}}(1 + \lambda \cdot K_{G_i}) - P_{L_{i0}}(1 + \lambda \cdot K_{L_i}) = V_i \sum_{j=1}^N V_j (G_{ij} \cos \delta_{ij} + B_{ij} \sin \delta_{ij}) \quad (i=1, \dots, N) \quad 11$$

$$Q_{G_{i0}} - Q_{L_{i0}}(1 + \lambda \cdot K_{L_i}) = V_i \sum_{j=1}^N V_j (G_{ij} \cos \delta_{ij} - B_{ij} \sin \delta_{ij}) \quad 12$$

where  $P_{L_{i0}}$  and  $Q_{L_{i0}}$  are the real and reactive base loads,  $P_{G_{i0}}$  and  $Q_{G_{i0}}$  are real and reactive base generation powers,  $\lambda$  is the load parameter variable representing an increased load percentage,  $\delta$  is the load angle between  $V_1$  and  $V_2$  and  $K_{L_i}$  and  $K_{G_i}$  are the constant multipliers to designate the change rates of load and generation respectively at bus  $i$  [14].

When  $\lambda = 0$ , it corresponds to the base load and when  $\lambda$  is increased to  $\lambda_{nose}$ , it corresponds to the critical load parameter condition (the collapse point).

**D. Steady State Stability Limit**

A stability limit is the maximum power flow possible through some particular point in the system, when the entire system or part of the system to which the stability limit refers is operating with stability [9]. Assume a small increment  $\Delta P$  in the electric power with the input from the prime mover remaining fixed at  $P_m$  causing the load angle to shift to  $\delta_0 + \Delta \delta$ , the change in electrical power can be written as;

$$\Delta P_e = \left( \frac{\partial P_e}{\partial \delta} \right)_0 \Delta \delta \quad 13$$

The system's response to small changes in MW loading is determined from the characteristic equation;

$$My^2 + \left[ \frac{\partial P_e}{\partial \delta} \right]_0 = 0 \quad 14$$

where  $M$  is the inertia constant and  $y_{1,2}$  are the roots of the equation [7].

Considering the two machine system is Figure 5, assuming  $V_1$  and  $V_2$  are constant, the system is stable if

$$\frac{V_1 V_2}{X} \cos \delta_0 < 0 \quad 15$$

The maximum power that can be transmitted below the critical load parameter occurs at  $\delta_0 = 90^\circ$  [7] therefore the steady state stability limit is given by

$$P_{max} = \frac{V_1 V_2}{X} \quad 16$$

E. Test Network and Simulation Environment

The methodological algorithms described are applied to the modified IEEE 14 Bus Network shown in Figure 6. The base network comprises of tap changing transformers and condensers which have been replaced with synchronous generators [10]. The network consists of five PV buses and eight PQ buses. Bus no 1 is taken as slack for convectional power flow evaluation.

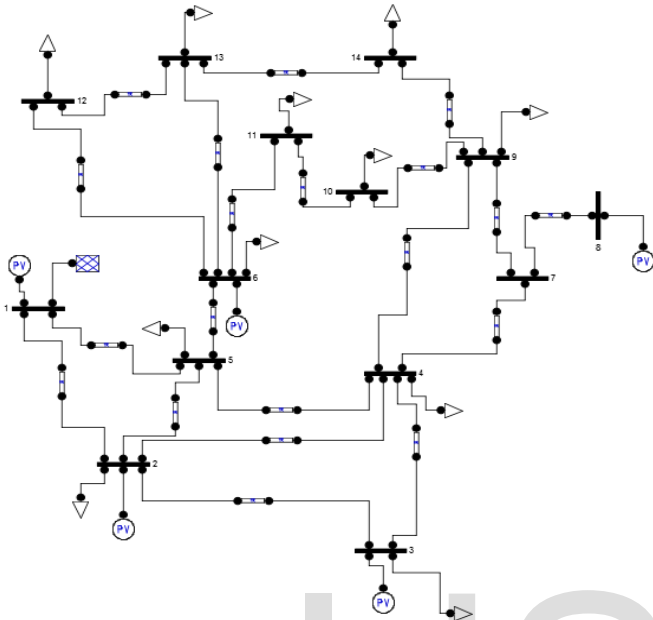


Figure 6 Modified IEEE 14 Bus System

The modified IEEE 14 bus network transmission line data in per unit is presented in Table 1.

Table 1 Transmission Line Data for the Test Network

From	To	Resistance p.u	Reactance p.u	Half Susceptance p.u
1	2	0.0194	0.0592	0.0264
2	3	0.0470	0.1980	0.0219
2	4	0.0581	0.1763	0.0187
1	5	0.0540	0.2230	0.0246
2	5	0.0570	0.1739	0.0170
3	4	0.0670	0.1710	0.0173
4	5	0.0134	0.0421	0.0064
5	6	0.0000	0.2520	0.0000
4	7	0.0000	0.2091	0.0000
7	8	0.0000	0.1762	0.0000
4	9	0.0000	0.5562	0.0000
7	9	0.0000	0.1100	0.0000
9	10	0.0318	0.0845	0.0000
6	11	0.0950	0.1989	0.0000
6	12	0.1229	0.2558	0.0000
6	13	0.0662	0.1303	0.0000
9	14	0.1271	0.2704	0.0000
10	11	0.0821	0.1921	0.0000
12	13	0.2209	0.1999	0.0000
13	14	0.1709	0.3480	0.0000

Table 2 presents the test network generation and load data as applied on PSAT 2.19 toolbox on MATLAB.

Table 2 Generator and Load Data for the Test Network

Bus No	Voltage Magnitude (p.u)	Load P (p.u)	Load Q (p.u)	Generation P (p.u)
1	1.05	0	0	0.8
2	1.05	0.3038	0.1778	0.8
3	1.04	1.3188	0.267	0.8
4	1	0.6691	0.1	0
5	1	0.1064	0.0224	0
6	1.05	0.1568	0.105	0.8
7	1	0	0	0
8	1.02	0	0	0.8
9	1	0.413	0.2324	0
10	1	0.126	0.0812	0
11	1	0.049	0.0252	0
12	1	0.0854	0.0224	0
13	1	0.189	0.0812	0
14	1	0.2086	0.07	0

PSAT software is a full-featured graphical power flow program to create, examine and modify the power flow data, solve the power flow, and view the solution reports [11]. The power flow data and solution are displayed in tables as well as on diagrams. The advantages of PSAT toolbox over other Matlab based applications are presented in Table 3 [8].

Table 3 Matlab Based Packages for Power System analysis

Package	PF	CPF	OPF	SSSA	TDS	EMT	GUI	CAD
EST	✓			✓	✓			✓
MatEMTP					✓		✓	✓
Matpower	✓		✓			✓		
PAT	✓			✓	✓			✓
PSAT	✓	✓	✓	✓	✓		✓	✓
PST	✓	✓		✓	✓			
SPS	✓			✓	✓	✓	✓	✓
VST	✓	✓		✓	✓		✓	

III RESULTS

A. Steady state operation

Figure 7 and 8 show the results of evaluation of the power flow of the modified IEEE 14 bus network to determine the bus voltages. It is seen that about 70% of bus voltage magnitudes lie within the acceptable and statutory voltage limit.

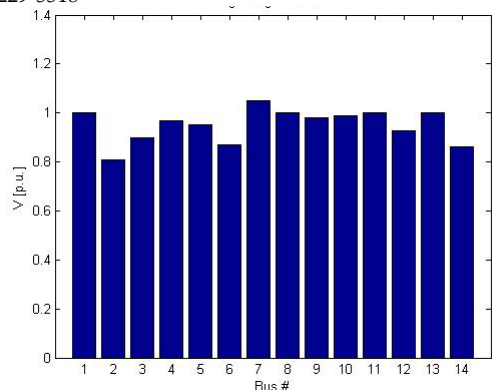


Figure 7 Bus Voltage Magnitude Profile

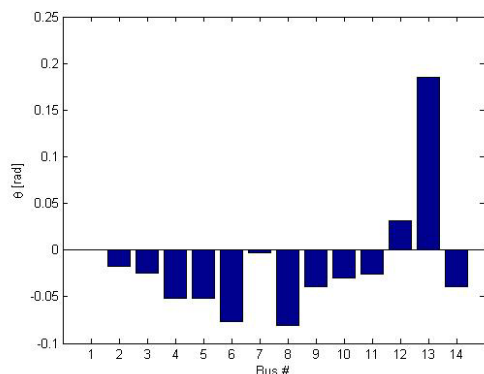


Figure 8 Bus Voltage Phase Angle

From Figure 8 which shows the bus voltage angle variations with respect to the reference bus no 1, it can be concluded that buses no 6, 8 and 13 are liable to experience voltage collapse even in the event of mild disturbances.

The real power generated and utilized by PV and PQ buses respectively is shown in Figure 9. The mean of 0.65p.u and 0.3p.u of power generation and power consumption was recorded for the network.

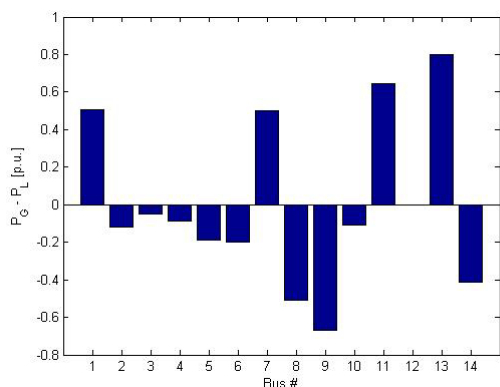


Figure 9 Active Power Magnitude

The relationship between reactive power and voltage magnitude at a PQ bus is justified by the result presented in Figure 10. Voltage instability being a local phenomenon, buses no 2 and 7 show to be critical buses that contribute a very high percentage to the voltage collapse of the network.

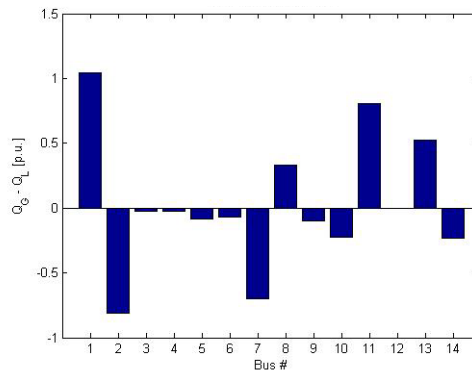


Figure 10 Reactive Power Magnitude

Table 4 shows the flow of active and reactive power for bus to bus and also the losses along the transmission lines. The highest active power loss is recorded from buses 10-11, 6-11, 10-11 and 9-10. Also large reactive power loss is recorded from buses 1-2, 6-11, 10-11, 9-10, 7-8, 7-9 and 4-7.

Table 1 Power Flow Result of Modified Network

From Bus	To Bus	P Flow [p.u.]	Q Flow [p.u.]	P Loss [p.u.]	Q Loss [p.u.]
2	1	-0.2903	-0.7631	0.0125	0.0105
2	3	0.3786	-0.0852	0.0070	0.0076
12	13	0.0401	0.0368	0.0007	0.0006
6	11	0.2019	0.4392	0.0222	0.0465
13	14	0.1406	0.1633	0.0088	0.0179
10	11	-0.1151	-0.3311	0.0157	0.0366
9	14	0.0699	-0.0717	0.0018	0.0037
10	9	-0.0049	-0.4789	0.0113	0.0301
4	9	-0.0007	0.1994	0.0000	0.0236
4	7	-0.3002	0.2371	0.0000	0.0327
7	8	-0.8000	-0.3613	0.0000	0.1607
7	9	0.4998	0.5658	0.0000	0.0743
3	4	-0.1384	0.2384	0.0054	-0.0030
2	4	0.2382	0.0982	0.0040	-0.0061
2	5	0.1735	0.0524	0.0019	-0.0108
5	4	0.2793	0.1897	0.0016	-0.0010
1	5	0.2057	0.2687	0.0060	-0.0007
5	6	-0.0141	-0.0812	0.0000	-0.0046
6	12	0.1277	0.0661	0.0025	0.0053
6	13	0.2995	0.2267	0.0093	0.0184

Figures 11 to 13 show the 3- dimensional visualization of the results of evaluation of the steady state power flow of the modified IEEE 14 bus test system. The hot spots depict the network areas with network parameters; voltage, voltage angle and current beyond stability limits.

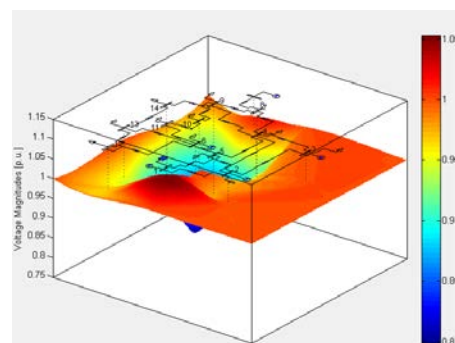


Figure 11 Bus Network Voltage Visualization



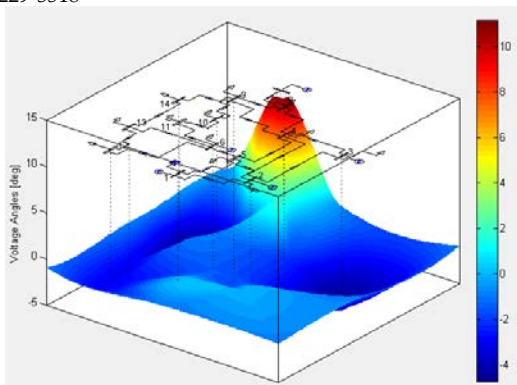


Figure 12 Bus Voltage Angles Visualization

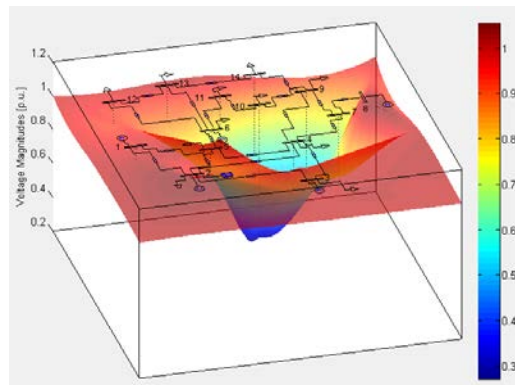


Figure 15 Bus Network Voltages Visualization with Slack bus 1

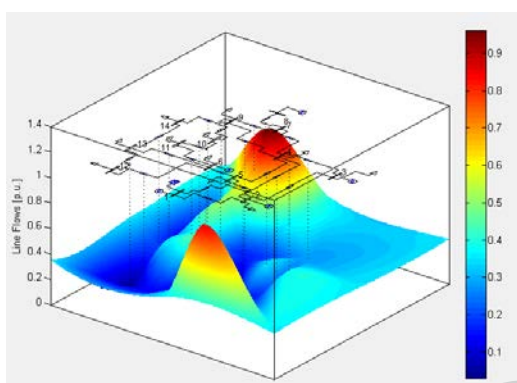


Figure 13 Network Line Current Flow Visualization

B. Total transfer capability and critical load parameter  
 Figures 14 to 18 show the results of implementation of continuous power flow algorithm to obtain the critical load parameter for the test network using bus no 1 as the slack.

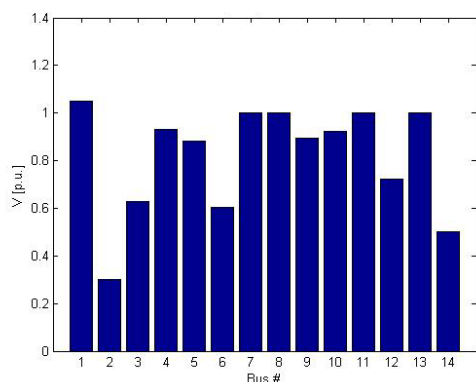


Figure 14 Bus Voltage Magnitude with Bus no 1 Slack

The bus voltage magnitudes visualization obtained using sparse matrix shows that bus no 2, 3, 6, 12 and 14 are critically low and are contributory to the high real and reactive power losses.

Improving the voltages at these buses through the addition of FACTS devices and on load tap changer transformers would increase the critical load parameter thereby increasing the steady state stability limit of the network. The network bus voltage magnitude with respect to slack bus no 1 is presented in Figure 16. Bus no 7 and 12 shows to be stable compared to every other PQ buses.

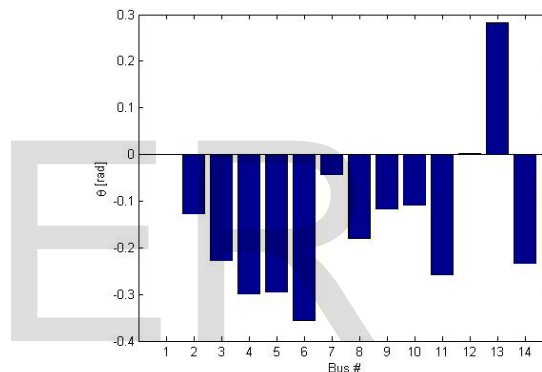


Figure 16 Voltage Phase Angle with Slack 1

Figure 17 shows the result of investigation of the critical load parameter of the modified IEEE 14 bus network model. Using PV bus no 1 as slack, the maximum load parameter beyond which secured steady state operation is jeopardized is 1.52p.u.

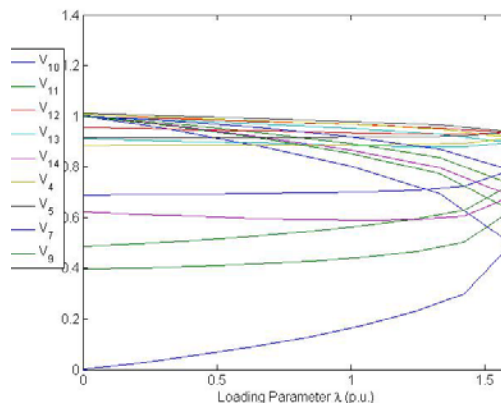


Figure 17 Critical Load Parameter with Slack Bus 1

The evaluation of the load parameter using the P-V curve method of the network under various slack buses is presented in Figure 18.

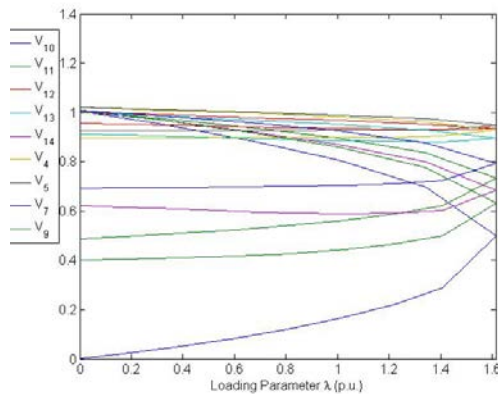


Figure 18 Critical Load Parameter with Slack 2

It is observed that the critical load parameter for the modified IEEE 14 bus network using buses 2, 3, 6 and 8 is 1.61p.u respectively.

The Power angle curve showing the maximum transferrable power under steady state operation also known as the steady state stability limit  $P_{max}$  corresponding to the critical voltage and critical load parameter, the steady state stability margin and current system loading is shown in Figure 18.

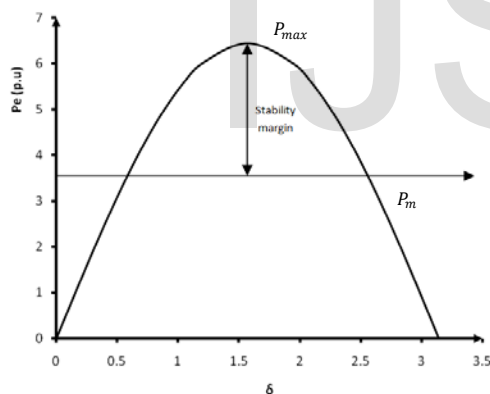


Figure 18 Power Angle Curve

The steady state stability margin of a network must be large enough to allow for maintenance of stability under steady and small disturbances so as to preclude the events of voltage collapse.

#### IV CONCLUSIONS

The cost of power system blackouts is immeasurable. Therefore the need to be able to maintain the operations of power systems within the normal and alert states by prevent voltage collapse is crucial. This paper investigated the critical load parameter for a modified IEEE 14-bus network under steady state operation using several slack bus scenarios. The stability margin of the system under steady

state operation is evaluated to be 46% well above the 20% minimum recommended margin for the maintenance of stability has been represented on the stability envelope. Conclusively, the stability margin and the critical load parameter moves in the same direction therefore methods to improve the index should be implemented.

#### V REFERNCES

- [1] Ajarapu, V. (2006). *Computational Techniques for Voltage Stability Assessment and Control*. New York: Springer.
- [2] Cutsem, T. V., & Vournas, C. (2008). *Voltage Stability of Electric Power Systems*. New York: Springer.
- [3] Debapriya, D. (2006). *Electrical Power Systems*. New Delhi: New Age International Publishers.
- [4] Gonen, T. (2012). *Electrical Machines with MATLAB*. London: CRC Press.
- [5] Hadi, S. (1999). *Power System Analysis*. New York: McGraw-Hill.
- [6] James, A. M. (2001). *Electric Power System Applications of Optimization*. New York: Marcel Dekker Inc.
- [7] Kothari, D. P., & Nagrath, I. J. (2008). *Power System Engineering* (Third ed.). New Delhi: McGraw Hill Education.
- [8] Milano, F. (2006). *Power System Analysis Toolbox*. Italy: Federicp Milano.
- [9] Murthy, P. (2007). *Power System Analysis*. Sultan Bazar: Adithya Art Printers, BS Publications, .
- [10] Parul, A. U., & Dharmeshkumar, P. (2013). Voltage Stability Assessment Using Continuation Power Flow. *International Journal of Advanced Research in Electrical, Electronics and Instrumentation Engineering* , 4017.
- [11] Powertech Labs Inc. (2011). *PSAT; Powerflow & Short-Circuit Analysis Tool*. British Columbia: Powertech Labs Inc.
- [12] Prabha, K. (1994). *Power System Stability and Control*. (J. B. Neal, & G. L. Mark, Eds.) New Jersey: McGraw Hills Inc.
- [13] Prabha, K., John, P., Venkat, A., & Göran, A. (2004, July). IEEE Transactions On Power Systems - Definition and Classification of Power System Stability. *IEEE/CIGRE Joint Task Force on Stability Terms and Definitions* , pp. 1-15.
- [14] Wenyuan, L. (2011). *Probabilistic Transmission System Planning*. New Jersey: John Wiley & Sons Inc Publication.